

Title: Reversible adipose tissue enlargement induced by external tissue suspension: possible contribution of basic fibroblast growth factor in the preservation of enlarged tissue

Harunosuke Kato, M.D.,^a Hirotaka Suga, M.D.,^a Hitomi Eto, M.D.,^a Jun Araki, M.D.,^a Noriyuki Aoi, M.D.,^a Kentaro Doi, M.D.,^a Takuya Iida, M.D.,^a Yasuhiko Tabata, Ph.D.,^b Kotaro Yoshimura, M.D.^{a*}

Institutions:

^a Department of Plastic Surgery, University of Tokyo, Tokyo, Japan

^b Department of Biomaterials, Institute for Frontier Medical Sciences, Kyoto University 53 Kawara-cho Seigoin, Sakyo-ku, Kyoto 606-8507, Japan.

Short running head: Tissue enlargement by external suspension

***Correspondence:**

Kotaro Yoshimura, M.D.

Department of Plastic Surgery, University of Tokyo School of Medicine, 7-3-1, Hongo, Bunkyo-Ku, Tokyo 113-8655, Japan.

TEL: +81-3-5800-8948

FAX: +81-3-5800-8947

E-mail: yoshimura-pla@h.u-tokyo.ac.jp

Grant numbers and sources of support: The authors declare that they have no competing financial interests. This work was supported by a grant from the Japanese Ministry of Education, Culture, Sports, Science, and Technology (MEXT); Contract grant numbers: B2- 19592070 and B2- 21592283.

Number of figures and tables: No table, 7 figures and 4 supplemental figures

Keywords:

- adipose-derived stromal cells

- adipose-derived stem cells
- gradual tissue expansion
- mechanotransduction
- external force
- basic fibroblast growth factor
- adipogenesis
- angiogenesis

ABSTRACT

Various kinds of tissue expansion have been performed clinically with internal devices, but external expansion has not previously been investigated. We applied continuous external force on skin tissue in a mouse model. Four weeks of external suspension caused enlargement of the subcutaneous tissue, particularly adipose tissue, though the enlargement was reversible. We found that the enlarged tissue volume could be adequately sustained with controlled release of basic fibroblast growth factor (bFGF), administered at the time the device was removed. Ki67+ proliferating cells, perilipin+ small adipocytes, lectin+ capillaries, and glycerol-3-phosphate dehydrogenase activity in the tissue increased during the expansion process, indicating dynamic adipose remodeling with adipogenesis and angiogenesis. Histological analyses revealed that vessels had elongated in the direction of the external force. Adipose-resident progenitor cells (adipose-derived stem/stromal cells) were the primary proliferating cell population involved in the remodeling process, particularly in the superficial layer. Treatment with b-FGF did not enhance the small adipocyte number, but promoted angiogenesis; this mechanism may contribute to the preservation of enlarged tissue. Our results suggested that external tissue suspension induced adipose tissue enlargement by activating resident progenitor cells and that this external suspension approach, combined with controlled release of bFGF, has therapeutic potential for soft tissue engineering.

INTRODUCTION

Gradual tissue expansion is a natural physiological phenomenon that occurs during growth, pregnancy, or morbid obesity; however, it is also an established therapeutic method for treating tissue defects. Tissue expansion is applied therapeutically with specific devices, including an internal tissue expander or an internal/external distraction osteogenesis system. Distraction osteogenesis can elongate limbs,^{1,2} the cranial bone, or the maxillofacial bone³ without bone grafting; an internal tissue expander is widely used in tissue reconstruction to expand healthy skin or soft tissue adjacent to defects imparted by trauma or surgery, like those due to mastectomy.⁴⁻⁶ Thus, gradual tissue expansion has been widely used as a reliable way to regenerate tissue, and it is considered a viable alternative to transplantation. Tissue expansion procedures can expand the target tissue to over twice the volume of the original tissue. The expansion capacity is based on the potential of target tissues that can expand and regenerate, like the skin, bone, or soft tissues. The regenerating potential has been attributed to the number (density) and potential of resident stem/progenitor cells specific to each tissue; thus, irradiated tissue has a limited potential for expansion.

Recently, continuous external tissue expansion was attempted with a device called the Brava[®] (Brava LLC, Miami, FL).^{7,8} This proved to be a potent procedure for soft tissue enlargement. Its primary advantage, compared to other conventional tissue expansion procedures, is the external application, which obviates any surgical interventions.⁷⁻⁹ The device expands the skin and soft tissue by applying external negative pressure from the outside. Edematous change was induced in response to the pressure, and the

expansion effects could be reversed, but significant expansion effects may be achieved when the distractive force was continuously applied for a sufficient period of time.^{7,8}

An external force is transduced into cells and subcellular structures through various mechanical disturbances, including shear, stretch, tension, distraction, and compression. These mechanical disturbances are converted into biological signals by a series of mechanotransduction pathways.¹⁰ There are many different cellular responses to mechanical forces, and many different second messengers that mediate these responses, including integrins or cadherins.¹⁰ It has been shown that applied mechanical forces can affect tissue growth, cellular function, and even survival.¹¹⁻¹⁶ Moreover, physical interactions with the extracellular matrix can significantly influence stem cell behavior.¹⁷

Studies on gradual tissue expansion are scarce, and, to our knowledge, no experimental research has been reported for soft tissue expansion in response to an external force. Therefore, in this study, we created an original animal model to examine cellular events during gradual tissue expansion with external tissue suspension. In any organ, tissue-resident or circulation-derived stem/progenitor cells are involved in a variety of tissue growth, repair, regeneration, and remodeling processes. We hypothesized that tissue-resident stem/progenitor cells would play an important role in the expansion process. We sought to evaluate the therapeutic potential of external tissue suspension for soft tissue enlargement. In a preliminary study, we found that soft tissue, particularly adipose tissue, was expanded after 4-weeks of external suspension, but the expansion was not sustained over a long time. Therefore, we performed an additional experiment to evaluate the effect of administering controlled release basic fibroblast growth factor

(bFGF) on the expanded tissue in an effort to prevent reversal and preserve tissue enlargement. Adipose tissue is known to contain multipotent mesenchymal cells,^{18,19} also referred to as adipose-derived stem, stromal, or progenitor cells (ASC).^{20,21} Compared to bone marrow stem cells, adipose tissue mesenchymal stem cells are easier to isolate, require less invasive procedures, and provide higher cell yields. Thus, ASCs hold promise for therapeutic use in tissue engineering and regenerative medicine.²⁰ In this study, we also analyzed in detail the involvement of ASCs in the tissue expansion/remodeling process.

MATERIALS AND METHODS

Mouse models for external tissue suspension

Eight-week-old Balb/c nude mice were anesthetized with intraperitoneal pentobarbital (50 mg/kg weight), and the back skin (30 mm diameter) was placed under continuous suspension, as follows. A suspension device, originally prepared for this purpose (Hiroki Corp., Kanagawa, Japan), was placed on a designated site in the back (Fig. 1A). The device comprised a small round plate (8 mm diameter) with a durable thread attached, that was placed on the skin. A round, adhesive, 30 mm-diameter film was placed over the plate, and the thread was pulled through a hole in the middle of the film. The film adhered to the plate and the back skin; thus, a pull on the string lifted both the plate and the surrounding skin. A plastic cap was then placed over the skin, film, and plate, and the thread was pulled through a hole and attached at the top of the plastic cap (Supplementary Fig.1). Sufficient force was applied to cause suspension of the patch of skin in contact with the adhesive film. The applied suspension force was

measured with a tension gage (ST02, Sanko Seikohjo Co. Ltd., Tokyo, Japan) and was 1.64 ± 0.26 N (mean \pm SEM) immediately after device application. The adhesive film was exchanged every 5 days. The suspended skin and underlying soft tissue was harvested at days 0, 3, 7, 14, or 28 (n= 6 in each group). For the 42-day animals (n=12), one of two types of gelatin microspheres (see below) were injected into the subcutaneous tissue at the suspension site on day 28; then the suspension device was not applied between days 28 and day 42. The harvested tissue samples were weighed and subjected to the assays described below.

bFGF-incorporated gelatin microspheres

Gelatin microspheres that contained bFGF or vehicle alone were prepared with a modification of a previously described method.²² In brief, 2 mg of gelatin microspheres were mixed with 20 μ l phosphate buffered saline (PBS), with or without bFGF (0.1 μ g). To the resulting 20 μ l hydrogel, we added 80 μ l PBS, to obtain a 100 μ l hydrogel mixture, containing bFGF or vehicle alone. On day 28, the suspension device was removed, and the 100 μ l hydrogel was carefully injected into the back skin under anesthesia (n=6 in each group, with or without 0.1 μ g bFGF).

To confirm the location of injected gelatin microspheres, we prepared frozen sections of skin samples. The sections were stained with DAPI (Vectashield[®]; Vector Laboratories, Burlingame, CA) to visualize nuclei under a fluorescence microscope (BioZero[®]; Keyence, Tokyo, Japan).

Glycerol-3-phosphate dehydrogenase (GPDH) assay

A GPDH Assay Kit (Cell Garage, Tokyo, Japan) was used to detect changes associated with adipocyte amount. The protocol was supplied by the manufacturer. In brief, harvested skin samples were submerged in 5 ml of a 0.25 M sucrose solution. The mixture was homogenized and then centrifuged at $430 \times g$ for 5 minutes. A 1 ml aliquot of the aqueous layer was obtained, and this was centrifuged at $17,700 \times g$ for 5 minutes. Next, the supernatant was diluted 10 \times with an enzyme-extracting reagent, the mixture was dispensed into the wells of a 96-well plate, two volumes of a substrate reagent was added, and the optical absorption was measured at 340 nm for 10 minutes. GPDH activity was calculated based on the following formula: $\text{GPDH (U/ml)} = \Delta\text{OD} \times 0.482 \times 5$ (ΔOD is the change in optical density per minute).

Whole mount staining of living subcutaneous adipose tissue

Visualization of living skin and subcutaneous tissue was performed with the procedure described by Nishimura et al.²³ Briefly, harvested skin samples were cut into 3 mm pieces within 2 hours after sacrifice, and the samples were incubated with the following reagents for 30 min: BODIPYTM 558/568 (dilution 1:100, Molecular Probes, Eugene, OR) to stain adipocytes, Alexa FluorTM 488-conjugated isolectin GS-IB₄ (dilution 1:200, Molecular Probes, Eugene, OR) to stain endothelial cells, and Hoechst 33342 (dilution 1:200, Dojindo, Kumamoto, Japan) to stain nuclei. The samples were then washed and directly observed with a confocal microscope system (Leica TCS SP2, Leica Microsystems GmbH, Wetzlar, Germany). Fifteen images, acquired at 2 μm intervals, were used for reconstructing a 30 μm -thick, three-dimensional image.

Immunohistochemistry

Harvested skin samples were paraffin-embedded. We prepared 6- μm -thick sections and performed immunostaining with the following primary antibodies: goat anti-mouse CD34 (dilution 1:100, Santa Cruz Biotechnology, Santa Cruz, CA), guinea pig anti-mouse perilipin (dilution 1:200, Progen, Heidelberg, Germany), and rabbit anti-human Ki67 (clone SP6, dilution 1:200, Thermo Fisher Scientific, Fremont, CA). For double fluorescence stains, the following secondary antibodies were used: Alexa FluorTM 488-conjugated donkey anti-goat IgG (dilution 1:200, Invitrogen, OR), Alexa FluorTM 488-conjugated goat anti-guinea pig IgG (dilution 1:200, Invitrogen), and Alexa FluorTM 594-conjugated donkey anti-rabbit IgG (dilution 1:200, Invitrogen). An isotypic antibody was used as a negative control for each antibody stain. Nuclei were stained with Hoechst 33342 (dilution 1:200, Dojindo). Blood vessels were stained with Lectin 488 (dilution 1:200, Invitrogen) or Isolectin 594 (dilution 1:200, Invitrogen). The number of capillaries (lectin+), proliferative ASCs (CD34+/Ki67+ nuclei), and small adipocytes (perilipin+ and less than 30 μm in diameter) were counted by analyzing at least 3 field images for each sample at low magnification.

Histological detection of apoptosis

To detect apoptosis in subcutaneous adipose tissue, terminal deoxynucleotidyl transferase dUTP nick-end labeling (TUNEL) was performed with an In-Situ Cell Death Detection Kit (Roche Diagnostics, Mannheim, Germany). The protocol was provided by the manufacture.

Statistical analysis

Results are expressed as mean \pm S.D. The statistical significance was determined using a Welch's *t*-test for all variables. Values of $p < 0.05$ were considered significant.

RESULTS

Macroscopic and weight changes of suspended tissue samples

After 28 days of continuous tissue suspension, the back skin appeared thickened and wrinkled, with a thick subcutaneous layer that appeared reddish, probably due to an increase in vasculature, while the skin was flat with a thin, pale-colored subcutaneous fatty layer at baseline (Fig. 1B). The weight of the suspended tissue increased with time and reached maximum enlargement on day 28. However, the weight was substantially lower on day 42, 14 days after removing the suspension device (Fig. 1C).

On day 28, the suspension device was removed, and gelatin microspheres containing bFGF or vehicle were injected into the expanded subcutaneous tissue. The presence of microspheres in the subcutaneous adipose tissue was confirmed by visualization with a fluorescence microscope (Supplemental online Fig. 2A). On day 42, the weights of harvested skin samples that were treated with bFGF microspheres were significantly higher (0.600 ± 0.045 g, $n=5$) than the control skin weights (0.371 ± 0.016 g, $n=6$) (Fig. 1C).

Histological and adipose volume (GPDH activity) changes in suspended tissues

Hematoxylin and eosin stained sections of tissues harvested during continuous suspension through day 28 showed a thickening of subcutaneous adipose tissue and muscle layers; in particular, an enlargement of the adipose tissue was noted (Fig. 2A).

On days 3 and 7, small-sized adipocytes appeared throughout the subcutaneous adipose

tissue, suggesting ongoing adipogenesis. After removing the suspension device on day 28, the thickened subcutaneous tissue shrank substantially, as noted on day 42 (Fig. 2A).

GPDH activity is known to increase when preadipocytes differentiate into adipocytes. We found that GPDH activity was elevated in the tissue samples from day 3 to day 28, but then declined on day 42 (Fig. 2B). The decline in GPDH on day 42 was partly prevented by administration of bFGF microspheres (0.101 ± 0.016 U/g, $n=3$) compared to controls (0.080 ± 0.008 U/g, $n=3$), but the difference was not statistically significant.

These results suggested that the volume of subcutaneous adipose tissue increased under continuous external suspension and reversed after releasing the suspension. Moreover, the treatment with bFGF contributed to preservation of the enlarged adipose tissue.

Cellular events evaluated by whole mount staining

Triple-fluorescence staining allowed three-dimensional analysis. Whole mount specimens were immediately stained without any fixing or sectioning procedures; thus, the obtained images reflected the original tissue structures, including adipocytes and capillaries. The reversible enlargement of subcutaneous adipose tissues by external tissue suspension was assessed by the whole mount histology (Fig. 3A). At baseline, capillaries or vessels ran between mature adipocytes of relatively similar cell size (40-60 μm diameters). On days 3, 7, and 14, small adipocytes were frequently observed among the mature adipocytes. On day 14, preadipocytes that contained multiple lipid droplets in the cytoplasm, were occasionally observed along capillaries (Supplemental online Fig. 2B). At baseline, the capillaries ran alongside adipocytes and formed a

well-organized network. On days 7, 14, and 28, capillaries appeared elongated, distended in the direction of the external suspension. In the group treated with bFGF microspheres, the enlarged fat tissue volume was retained compared to the control group, and the increased density of vascular structures was also relatively preserved (Fig. 3B).

Increased number of small adipocytes under suspension

Small adipocytes, suggesting ongoing adipogenesis, were counted in microsections stained for perilipin (Fig. 4A). Under external suspension, the number of small adipocytes increased and peaked on day7; thereafter, it declined to the baseline level on day28, and treatment with bFGF-incorporated microspheres did not influence the number (Fig. 4B).

Increased number of capillaries in subcutaneous adipose tissue

Lectin-positive capillaries increased in number under tissue suspension and peaked on day 7 (Fig. 5A). On day 42, the number of capillaries in subcutaneous adipose tissue treated with bFGF (38 ± 13) was significantly higher than that of controls (15 ± 3) (Fig. 5B). These results suggested that angiogenesis was associated with adipogenesis under external tissue suspension.

Proliferating cells in subcutaneous adipose tissue under suspension

Histological analysis of day 14 samples showed that most Ki67+ proliferating cells were CD34+ and lectin-, which suggested that they were ASCs (Figs. 6A, 6B). CD34+ ASCs increased in number and were most frequently observed in the superficial adipose layer immediately under the dermis. Lectin+/CD34+ cells were also

occasionally observed, perhaps due to the transdifferentiation of cells from ASCs to vascular endothelial cells (Fig. 6C). The Lectin+/CD34+ cells were most frequently observed on day 14 (Supplementary Fig. 3).

Sequential changes in the frequency of CD34+/Ki67+ cells (proliferating ASCs) was measured during external suspension (Fig. 7A). The frequency started to increase on day 7; this suggested a regenerating process like adipogenesis and/or angiogenesis due to external suspension (Fig. 7B). On day 42, the percentage of CD34+/Ki67+ cells was higher in the adipose tissue treated with bFGF (11.2 ± 3.3 %) microspheres than in the controls (8.6 ± 1.5 %) ($p=0.06$; $n=3$).

Apoptosis in subcutaneous adipose tissue after releasing suspension

To examine acute changes after removing the suspension device, some samples were harvested on day 29. The enlarged tissues showed acute shrinking, and TUNEL-positive nuclei were frequently observed (Supplemental online Figs. 4A, 4B). Fewer TUNEL-positive nuclei were observed on day 42 (data not shown), suggesting that apoptosis may be one of the mechanisms driving the reversal of enlargement in the adipose tissue volume.

DISCUSSION

Our results showed that application of continuous external suspension induced soft tissue enlargement, particularly in the subcutaneous adipose layer. However, the enlargement was reversible as far as external suspension was applied for up to 4 weeks.

This reversible enlargement was also observed in a clinical trial with an external expansion device.⁹ From days 14 to 28, the skin samples showed increases in weight, GPDH, and capillary density, which almost reached a plateau; the interstitial space had decreased and each emerging adipocyte appeared to be mature by 28 days. The tissue shrinkage after discontinuation of the external force suggested that the augmented volume may have been partly due to interstitial fluid pooling (edema), though the histological findings did not clearly indicate edema and GPDH activity was increased after tissue suspension. Our results suggested that apoptosis of adipocytes may be one of the mechanisms underlying the reversal of enlarged tissue volume. The animal model used in this study was novel, because previously, no animal models existed for non-obese adipose tissue enlargement or for experimental external tissue expansion.

This study also showed that the reversal of enlarged soft tissue may be prevented by a concomitant use of controlled release growth factors, like bFGF. This suggested that a combined use of external expansion and growth factors is a potential therapeutic strategy. It has been shown that adipogenesis requires accompanying angiogenesis,²⁴ and the extent of angiogenesis may determine the partial pressure of tissue oxygen and affect metabolic functions of the generated adipocytes. Capillaries increased in density during the angiogenesis process, and also after treatment of bFGF along with discontinuation of external suspension.

During the 4-week expansion period, several dynamic cellular events were observed that were associated with tissue remodeling, including: the proliferation and differentiation of cells, like ASCs; angiogenic changes, including increased capillary density and elongation of vessels along the direction of tissue suspension; and

increased adipogenesis, suggested by the increased number of small adipocytes and the increase in GPDH activity. The histological results indicated that cell proliferation was promoted from day 7, and that the proliferating population primarily comprised ASCs (lectin⁻/CD34⁺). The role of ASCs in the adipogenesis/angiogenesis process was previously shown in the repair process after ischemia-reperfusion injury to adipose tissue.²⁵ Lectin⁺/CD34⁺ cells were also observed in the proliferative area; this suggested that ASCs may differentiate into lectin⁺/CD34⁻ vascular endothelial cells. There have been a number of studies that demonstrated the extraordinary proangiogenic potential of ASCs, and some have shown that ASCs had potential for differentiating into vascular endothelial cells. For example, implanted ASCs differentiated into endothelial cells and smooth muscle cells, which incorporated into newly formed vessels in several animal models, including carcinogenesis, ischemia, and an adipose graft model.²⁶⁻³⁰ However, ASC differentiation into endothelial cells may not occur at a high frequency.^{31,32}

A large body of evidence showed that soluble growth factors are released from ASCs and, in addition, can affect the behavior of ASCs. Among the growth factors tested, bFGF appeared to have the largest impact on ASC function and behavior. Basic FGF is released from injured tissue immediately after wounding³³ and has been reported to promote cell proliferation,³⁴ inhibit apoptosis, stimulate release of angiogenic growth factors, like hepatocyte growth factor (HGF),²⁵ and enhance adipogenic differentiation.³⁵ In vivo experiments showed subcutaneous implantation of Matrigel with control release of bFGF induced de novo adipogenesis.²³ In addition, bFGF enhanced ASC survival after transplantation, promoted blood perfusion and adipogenesis, and prevented fibrogenesis.^{25,29} This study showed that controlled release

bFGF improved the retention rate of enlarged adipose tissue after continued external tissue suspension. The numerical measurement of small adipocytes suggested that adipogenesis was not upregulated by bFGF. Therefore, the upregulation of angiogenesis and the suppression of adipocyte death may be a mechanism underlying the effect of bFGF on the preservation of adipose tissue volume. Adipocytes are very sensitive to hypoxia and undergo apoptosis under hypoxic conditions.³⁶ Therefore, the increased capillaries associated with bFGF treatment may have led to higher tissue oxygen levels in adipose tissue, and resulted in the prevention of hypoxia-induced adipocyte death.

In our animal model, the application of external suspension resulted in microdeformation of the tissue. This induced cell proliferation and angiogenesis, consistent with responses observed with vacuum assisted closure.³⁷ It has been shown that both not only soluble factors but also mechanical forces modulate stem cell behaviors; for example, the differentiation lineages of mesenchymal stem cells was determined by gradients of mechanical stress.³⁸ The interactions between cells and mechanical factors are critical to the health and function of various tissues and organs of the body and may play critical roles in controlling stem cell fate and lineage determination.¹⁷ There are a variety of mechanotransduction molecules that regulate stem cell differentiation, including the actin cytoskeleton, mechano- and osmotically sensitive ion channels, and chromatin remodeling enzymes.¹⁷ This study provides in vivo evidence that mechanical force was able to activate resident stem cells and induce dynamic tissue remodeling, accompanied by adipogenesis and angiogenesis, although the detailed mechanical transduction pathways remain to be definitively determined. Several phenomena observed in this study reflected influences of mechanical forces,

such as a higher density of proliferating cells in superficial layers and elongated vessels arranged parallel to the direction of the external force.

In conclusion, continuous external suspension for 4 weeks induced reversible tissue enlargement, particularly in adipose tissue. Adipose-resident progenitor cells (ASCs) were highly involved in the dynamic expansion/remodeling process; ASCs actively proliferated, differentiated, and contributed to adipogenesis and angiogenesis. Although discontinuation of the external force resulted in a reduction in the enlarged tissue volume, the enlarged tissue could be preserved and capillary density was increased by treatment of controlled release bFGF. These results suggested that an external force can induce soft tissue engineering with a clinically useful significance and the combination of tissue suspension with an external device and controlled release of bFGF has potential as a therapy for soft tissue expansion that does not require cell transplantation.

Acknowledgments

We thank Ayako Kurata for technical assistance. Recombinant human basic fibroblast growth factor was kindly provided by Kaken Pharmaceutical Co. Ltd. (Tokyo, Japan). Devices for the external suspension of mouse skin were manufactured and kindly provided by Hiroki Corp. (Yokohama, Japan).

REFERENCES

1. Herbert, A.J., Herzenberg, J.E., and Paley, D. A review for pediatricians on limb lengthening and the Ilizarov method. *Curr Opin Pediatr* 7, 98, 1995.
2. James, A. Limb-lengthening, skeletal reconstruction, and bone transport with the Ilizarov method. *J Bone Joint Surg Am* 79, 1243, 1997.
3. Matsumoto, K., Nakanishi, H., Kubo, Y., Yokozeki, M., and Moriyama, K. Advances in distraction techniques for craniofacial surgery. *J Med Invest* 50, 117, 2003.
4. LoGiudice, J., and Gosain, A.K. Pediatric tissue expansion: indications and complications. *J Craniofac Surg* 14, 866, 2003.
5. Motamed, S., Niazi, F., Atarian, S., and Motamed, A. Post-burn head and neck reconstruction using tissue expanders. *Burns* 34, 878, 2008.
6. Spear, S.L., Newman, M.K., Bedford, M.S., Schwartz, K.A., Cohen, M., and Schwartz, J.S. A retrospective analysis of outcomes using three common methods for immediate breast reconstruction. *Plast Reconstr Surg* 122, 340, 2008.
7. Khouri, R.K., Schlenz, I., Murphy, B.J., and Baker, T.J. Nonsurgical breast enlargement using an external soft-tissue expansion system. *Plast Reconstr Surg* 105, 2500, 2000.
8. Schlenz, I., and Kaider, A. The Brava external tissue expander: is breast enlargement without surgery a reality? *Plast Reconstr Surg* 120, 1680, 2007.
9. Khouri, R., and Del Vecchio, D. Breast reconstruction and augmentation using pre-expansion and autologous fat transplantation. *Clin Plast Surg* 36, 269, 2009.
10. Chen, C.S. Mechanotransduction a field pulling together? *J Cell Sci* 121, 3285, 2008.
11. Chen, C.S., Mrksich, M., Huang, S., Whitesides, G.M., and Ingber, D.E. Geometric control of cell life and death. *Science* 276, 1425, 1997.

12. Millward-Sadler, S.J.M., and Salter, D.M. Integrin-dependent signal cascades in chondrocyte mechanotransduction. *Ann Biomed Eng* 32, 435, 2004.
13. Humphrey, J.D. Vascular adaptation and mechanical homeostasis at tissue, cellular, and sub-cellular levels. *Cell Biochem Biophys* 50, 53, 2008.
14. Dahl, K.N., Ribeiro, A.J.S., and Lammerding, J. Nuclear shape, mechanics, and mechanotransduction. *Circ Res* 102, 1307, 2008.
15. Alomruiz, S., and Chen, C.S. Emergence of patterned stem cell differentiation within multicellular structures. *Stem Cells* 26, 2921, 2008.
16. Riddle, R.C., and Donahue, H.J. From streaming potentials to shear stress: 25 years of bone cell mechanotransduction. *J Orthop Res* 27, 143, 2009.
17. Guilak, F., Cohen, D.M., Estes, B.T., Gimble, J.M., Liedtke, W., and Chen, C.S. Control of stem cell fate by physical interactions with the extracellular matrix. *Cell Stem Cell* 5, 17, 2009.
18. Zuk, P.A., Zhu, M., Ashjian, P., Ugarte, D.A.D., Huang, J.I., Mizuno, H., Alfonso, Z.C., Fraser, J.K., Benhaim, P., and Hedrick, M.H. Human adipose tissue is a source of multipotent stem cells. *Mol Biol Cell* 13, 4279, 2002.
19. Rodeheffer, M.S., Birsoy, K., and Friedman, J.M. Identification of white adipocyte progenitor cells in vivo. *Cell* 135, 240, 2008.
20. Gimble, J.M., Katz, A.J., and Bunnell, B.A. Adipose-derived stem cells for regenerative medicine. *Circ Res* 100, 1249, 2007.
21. Yoshimura, K., Shigeura, T., Matsumoto, D., Sato, T., Takaki, Y., Aiba-Kojima, E., Sato, K., Inoue, K., Nagase, T., Koshima, I., and Gonda, K. Characterization of freshly isolated and cultured cells derived from the fatty and fluid portions of liposuction aspirates. *J Cell Physiol* 208, 64, 2006.

22. Tabata, Y., Miyao, M., Inamoto, T., Ishii, T., Hirano, Y., Yamaoki, Y., and Ikada, Y. *De novo* formation of adipose tissue by controlled release of basic fibroblast growth factor. *Tissue Eng* 6, 279, 2000.
23. Nishimura, S., Manabe, I., Nagasaki, M., Hosoya, Y., Yamashita, H., Fujita, H., Ohsugi, M., Tobe, K., Kadowaki, T., Nagai, R., and Sugiura, S. Adipogenesis in obesity requires close interplay between differentiating adipocytes, stromal cells, and blood vessels. *Diabetes* 56, 1517, 2007.
24. Cao, Y. Angiogenesis modulates adipogenesis and obesity. *J Clin Invest* 117, 2362, 2007.
25. Suga, H., Eto, H., Shigeura, T., Inoue, K., Aoi, N., Kato, H., Nishimura, S., Manabe, I., Gonda, K., and Yoshimura, K. IFATS collection: Fibroblast growth factor-2-induced hepatocyte growth factor secretion by adipose-derived stromal cells inhibits postinjury fibrogenesis through a c-Jun N-terminal kinase-dependent mechanism. *Stem Cells* 27, 238, 2009.
26. Benard, V.P., Silvestre, J.S., Cousin, B., Andre, M., Nibbelink, M., Tamarat, R., Clergue, M., Manneville, C., Barreau, C.S., Dueiz, M., Tedgui, A., Levy, B., Penicaud, L., and Casteilla, L. Plasticity of human adipose lineage cells toward endothelial cells: physiological and therapeutic perspectives. *Circulation* 109, 656, 2004.
27. Miranville, A., Heeschen, C., Sengenès, C., Curat, C.A., Busse, R., and Bouloumié, A. Improvement of postnatal neovascularization by human adipose tissue-derived stem cells. *Circulation* 110, 349, 2004.
28. Matsumoto, D., Sato, K., Gonda, K., Takaki, Y., Shigeura, T., Sato, T., Aiba, E., Iizuka, F., Inoue, K., Suga, H., and Yoshimura, K. Cell-assisted lipotransfer: supportive use of human adipose-derived cells for soft tissue augmentation with lipoinjection. *Tissue Eng* 12, 3375, 2006.

29. Bhang, S.H., Cho, S.W., Lim, J.M., Kang, J.M., Lee, T.J., Yang, H.S., Song, Y.S., Park, M.H., Kim, H.S., Yoo, K.J., Jang, Y., Langer, R., Anderson, D.G., and Kim, B.S. Locally-delivered growth factor enhances the angiogenic efficacy of adipose-derived stromal cells transplanted to ischemic limbs. *Stem Cells*, in press (doi: 10.1002/stem.115)
30. Muehlberg, F.L., Song, Y.H., Krohn, A., Pinilla, S.P., Droll, L.H., Leng, X., Seidensticker, M., Ricke, J., Altman, A.M., Devarajan, E., Liu, W., Arlinghaus, R.B., and Alt, E.U. Tissue-resident stem cells promote breast cancer growth and metastasis. *Carcinogenesis* 30, 589, 2009.
31. Nakagami, H., Maeda, K., Morishita, R., Iguchi, S., Nishikawa, T., Takami, Y., Kikuchi, Y., Saito, Y., Tamai, K., Ogihara, T., and Kaneda, Y. Novel autologous cell therapy in ischemic limb disease through growth factor secretion by cultured adipose tissue-derived stromal cells. *Arterioscler Thromb Vasc Biol* 25, 2542, 2005.
32. Rubina, K., Kalinina, N., Efimenko, A., Lopatina, T., Melikhova, V., Tsokolaeva, Z., Sysoeva, V., Tkachuk, V., and Parfyonova, Y. Adipose stromal cells stimulate angiogenesis via promoting progenitor cell differentiation, secretion of angiogenic factors, and enhancing vessel maturation. *Tissue Eng Part A*, in press (doi: 10.1089=ten.tea.2008.0359)
33. Aiba-Kojima, E., Tsuno, N.H., Inoue, K., Matsumoto, D., Shigeura, T., Sato, T., Suga, H., Kato, H., Nagase, T., Gonda, K., Koshima, I., Takahashi, K., and Yoshimura, K. Characterization of wound drainage fluids as a source of soluble factors associated with wound healing: comparison with platelet-rich plasma and potential use in cell culture. *Wound Rep Reg* 15, 511, 2007.

34. Suga, H., Shigeura, T., Matsumoto, D., Inoue, K., Kato, H., Aoi, N., Murase, S., Sato, K., Gonda, K., Koshima, I., and Yoshimura, K. Rapid expansion of human adipose-derived stromal cells preserving multipotency. *Cytotherapy* 9, 738, 2007.
35. Kakudo, N., Shimotsuma, A., and Kusumoto, K. Fibroblast growth factor-2 stimulates adipogenic differentiation of human adipose-derived stem cells. *Biochem Biophys Res Commun* 359, 239, 2007.
36. Yoshimura, K., Suga, H., and Eto, H. Adipose-derived stem/progenitor cells: roles in adipose tissue remodeling and potential use for soft tissue augmentation. *Regen Med* 4, 265, 2009.
37. Orgill, D.P., Manders, E.K., Sumpio, B.E., Lee, R.C., Attinger, C.E., Gurtner, G.C., and Ehrlich, H.P. The mechanisms of action of vacuum assisted closure: more to learn. *Surgery* 146, 40, 2009.
38. Alomruiz, S., and Chen, C.S. Emergence of patterned stem cell differentiation within multicellular structures. *Stem Cells* 26, 2921, 2008.

FIGURE LEGENDS**Figure 1.** Tissue enlargement by continuous suspension

(A) Suspension device applied on the back skin. The skin was continuously suspended with a device specifically prepared for this purpose (see Supplementary Fig. 1 for details). (B) Macroscopic views of tissue samples harvested on days 0 and 28. Cross sectional (left), external (middle), and internal (right) views of representative tissue samples. Substantial increases in skin thickness and vascular density were noted after continuous suspension for 28 days. (C) Weight changes of harvested tissue samples. The weight of the samples increased during tissue suspension until day 28, but the increased weight was lost 14 days after discontinuing the suspension. However, administration of bFGF microspheres on day 28 preserved the tissue enlargement and these samples showed significantly higher tissue weights than the controls on day 42. Data are shown as mean + SD. * $p < 0.05$.

Figure 2. Histological and GPDH activity changes in suspended tissue

(A) Histological views (hematoxylin and eosin staining) of suspended skin samples on days 0, 3, 7, 14, 28, and 42 at low (left column) or high (right column) magnification. The subcutaneous layer, particularly the adipose layer, expanded over time from day 0 to day 28. On the other hand, the expanded subcutaneous adipose tissue shrunk on day 42, 14 days after the discontinuation of tissue suspension. Scale bars = 200 μm (left) or 50 μm (right). (B) GPDH activity of tissue samples. GPDH activity, reflecting adipose tissue volume, increased with continuous suspension, but returned to baseline by day 42. Administration of bFGF microspheres caused less reduction of GPDH, though this did not reach statistical significance.

Figure 3. Whole mount histology of tissue samples

Harvested tissue was stained with BODIPY (adipocytes; green), lectin (endothelial cells; red), and Hoechst 33342 (nuclei; blue). **(A)** Suspended tissue samples at low (left column) or high (right column) magnification. With continuous suspension, the subcutaneous adipose layer thickened; numerous new capillaries formed in the adipose tissue and growth extended in the direction of the applied force. Scale bars = 200 μm (left column) or 25 μm (right column). **(B)** Tissue samples on day 42. The enlarged subcutaneous adipose tissue had shrunken by day 42 in controls; however, the administration of bFGF-incorporated microspheres was associated with a thicker layer of adipose and more prominent capillary network compared to the control. Scale bars = 200 μm (left column) or 25 μm (right column).

Figure 4. Measurement of small adipocytes in samples immunostained for perilipin.

(A) Histological sections immunostained for perilipin (plasma membrane of viable adipocytes; green), or stained with lectin (endothelial cells; red) and Hoechst 33342 (nuclei; blue). Scale bars = 50 μm . **(B)** Sequential change in the number of small adipocytes. The numbers of small adipocytes (diameter of less than 30 μm) per optical field were counted. The number of small adipocytes, reflecting ongoing adipogenesis, peaked on day 7.

Figure 5. Histological measurement of vasculature in tissue samples

(A) Histology of subcutaneous adipose tissue stained with lectin (endothelial cells; red) and Hoechst 33342 (nuclei; blue). Tissue was harvested on days 0, 3, 7, 14, and 28; some animals were removed from the suspension device and samples were harvested

14 days later (day 42). Some animals received bFGF-incorporated microspheres after removal of the suspension device, and then samples were harvested on day 42. Scale bars = 25 μm . **(B)** Quantification of vessels in the subcutaneous adipose tissue. The number of vessels per field was counted in images at a low magnification. The largest number of vessels was observed on day 7. A larger number of vessels were counted in bFGF-treated tissues compared to the control on day 42 (* $p < 0.05$).

Figure 6. Immunohistological analysis of proliferating cells in tissues under suspension

(A) Tissue samples harvested on day14 were triply stained with anti-Ki67 (proliferative cells; red), anti-CD34 (ASCs; green), and Hoechst 33342 (nuclei; blue). Most proliferating cells were CD34+, suggesting that they were ASCs. Scale bars = 100 μm (yellow); boxed sections were enlarged at 10 μm (white). **(B)** Tissue samples harvested on day14 were triply stained with lectin (capillaries; red), anti-Ki67 (proliferative cells; green), and Hoechst 33342 (nuclei; blue). Most of proliferating cells were lectin-, which also suggested that they were ASCs. Scale bars = 100 μm (yellow); boxed section was enlarged at 25 μm (white). **(C)** Tissue samples harvested on day14 were triply stained with lectin (capillaries; red), anti-CD34 (ASCs; green), and Hoechst 33342 (nuclei; blue). CD34+ cells were most frequently observed in the superficial adipose layer, immediately under the dermis. In that area, there were lectin+/CD34- endothelial cells (red arrow heads), lectin-/CD34+ ASCs (green arrow heads), and also lectin+/CD34+ cells (white arrow heads), which may be ASCs that are trans-differentiateing into vascular endothelial cells. Scale bars = 100 μm (yellow); boxed section was enlarged at 10 μm (white).

Figure 7. Histological measurement of proliferating ASCs in tissues under suspension

(A) Tissue samples harvested on days 0, 3, 7, 14, 28, and 42 were triply stained with anti-Ki67 (proliferative cells; red), anti-CD34 (ASCs; green), and Hoechst 33342 (nuclei; blue). Scale bars = 50 μ m (B) Quantification of CD34+/Ki67+ cells. The double positive cells (ASCs) increased in number from day 7 to day 28. The number of proliferating ASCs decreased after cessation of suspension, but the decrease appeared to be partly compensated by administration of bFGF.

Supplementary Figure 1. Suspension device

A suspension device specifically designed for this experiment (Hiroki Corp., Yokohama, Japan). An adhesive film (diameter =30 mm) combined with a plastic plate was placed on the back skin of mice. A suspension thread attached to the plate was threaded through the hole in a plastic cap placed over the plate. The thread was then pulled upward and fixed to the plastic cap to maintain a suspending force on the skin (see also Figure 1A). The suspension device was exchanged every 5 days throughout the experiment.

Supplementary Figure 2. The application of gelatin microspheres by subcutaneous injection. (A) Gelatin microspheres containing bFGF or PBS were subcutaneously injected on day 28, and tissue suspension was discontinued. A paraffin section of the harvested tissue was stained with DAPI (nuclei; blue) and the injected auto-fluorescent microspheres (yellow) were visualized under a fluorescence microscope. Scale bars = 100 μ m. (B) Preadipocytes observed under external suspension (day 14). Whole mounts were triply-stained with BODIPY (lipid; green), lectin (endothelial cells; red),

and Hoechst 33342 (nuclei; blue); preadipocytes located alongside the capillaries (red) contained numerous small lipid droplets (green). Scale bars = 5 μm .

Supplementary Figure 3. Tissue samples were triply-stained with lectin (capillaries; red), anti-CD34 (ASCs; green), and Hoechst 33342 (nuclei; blue).

Samples were harvested and stained on day 0, 3, 7, 14, and 28. Lectin+/CD34+ cells (white arrow heads), which may be cells that trans-differentiated from ASCs into vascular endothelial cells, were most frequently observed on day 14. Scale bars = 100 μm (yellow); boxed sections were enlarged at 25 μm (white).

Supplementary Figure 4. Histological section of tissue samples harvested on day 29

(A) Hematoxylin and eosin staining of a sample harvested on day 29, one day after removal of the suspension device. A substantial reduction in tissue volume was observed compared to day 28. Scale bar = 200 μm . (B) TUNEL staining of tissue samples harvested on day 29. TUNEL staining (left column) and the same image merged with DAPI nuclear staining (right column) showed apoptotic changes. Scale bars = 50 μm .

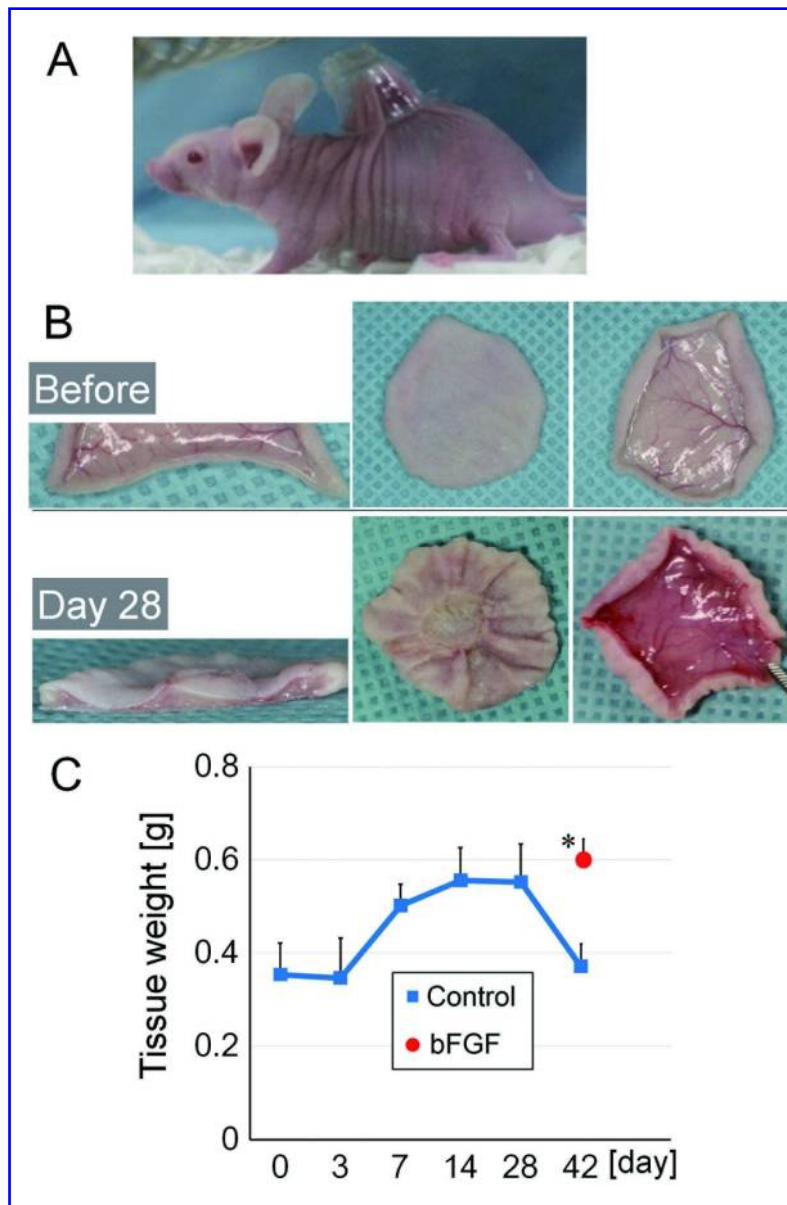


Figure 1. Tissue enlargement by continuous suspension
 (A) Suspension device applied on the back skin. The skin was continuously suspended with a device specifically prepared for this purpose (see Supplementary Fig. 1 for details). (B) Macroscopic views of tissue samples harvested on days 0 and 28. Cross sectional (left), external (middle), and internal (right) views of representative tissue samples. Substantial increases in skin thickness and vascular density were noted after continuous suspension for 28 days. (C) Weight changes of harvested tissue samples. The weight of the samples increased during tissue suspension until day 28, but the increased weight was lost 14 days after discontinuing the suspension. However, administration of bFGF microspheres on day 28 preserved the tissue enlargement and these samples showed significantly higher tissue weights than the controls on day 42. Data are shown as mean + SD. * $p < 0.05$.

148x225mm (300 x 300 DPI)

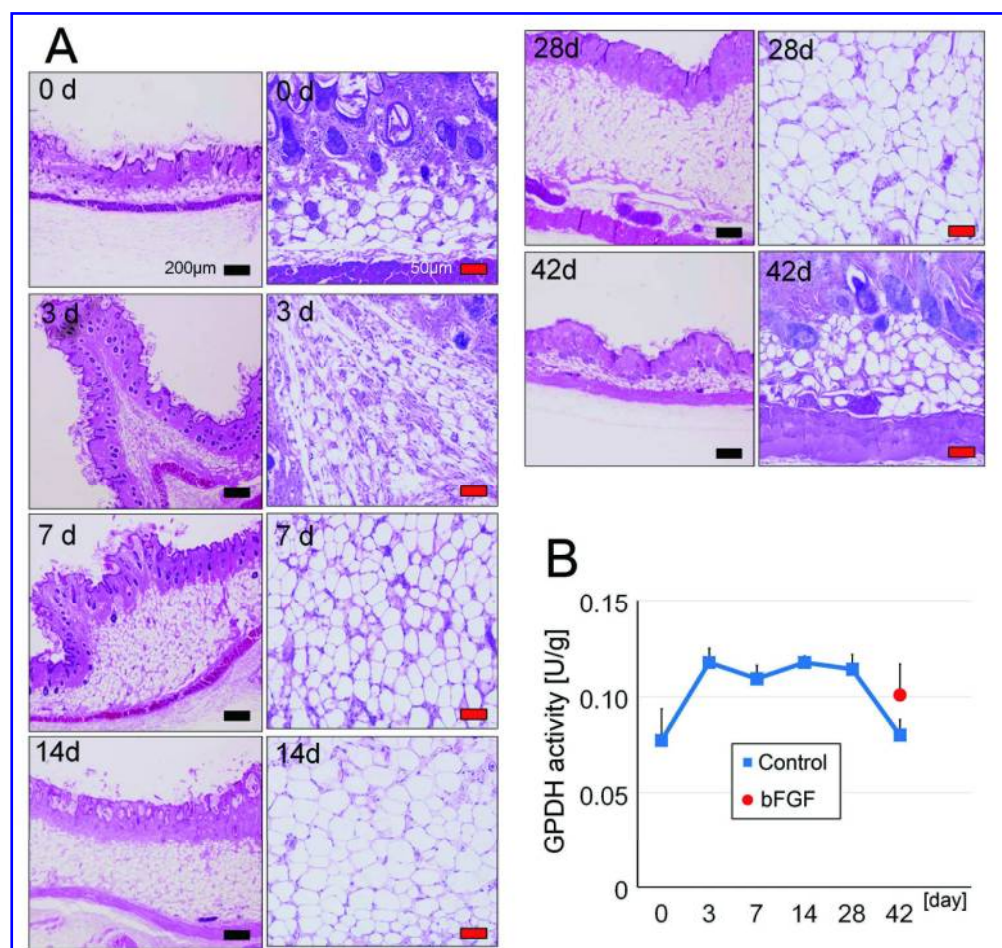


Figure 2. Histological and GPDH activity changes in suspended tissue
 (A) Histological views (hematoxylin and eosin staining) of suspended skin samples on days 0, 3, 7, 14, 28, and 42 at low (left column) or high (right column) magnification. The subcutaneous layer, particularly the adipose layer, expanded over time from day 0 to day 28. On the other hand, the expanded subcutaneous adipose tissue shrunk on day 42, 14 days after the discontinuation of tissue suspension. Scale bars = 200 µm (left) or 50 µm (right). (B) GPDH activity of tissue samples. GPDH activity, reflecting adipose tissue volume, increased with continuous suspension, but returned to baseline by day 42. Administration of bFGF microspheres caused less reduction of GPDH, though this did not reach statistical significance.

243x229mm (300 x 300 DPI)

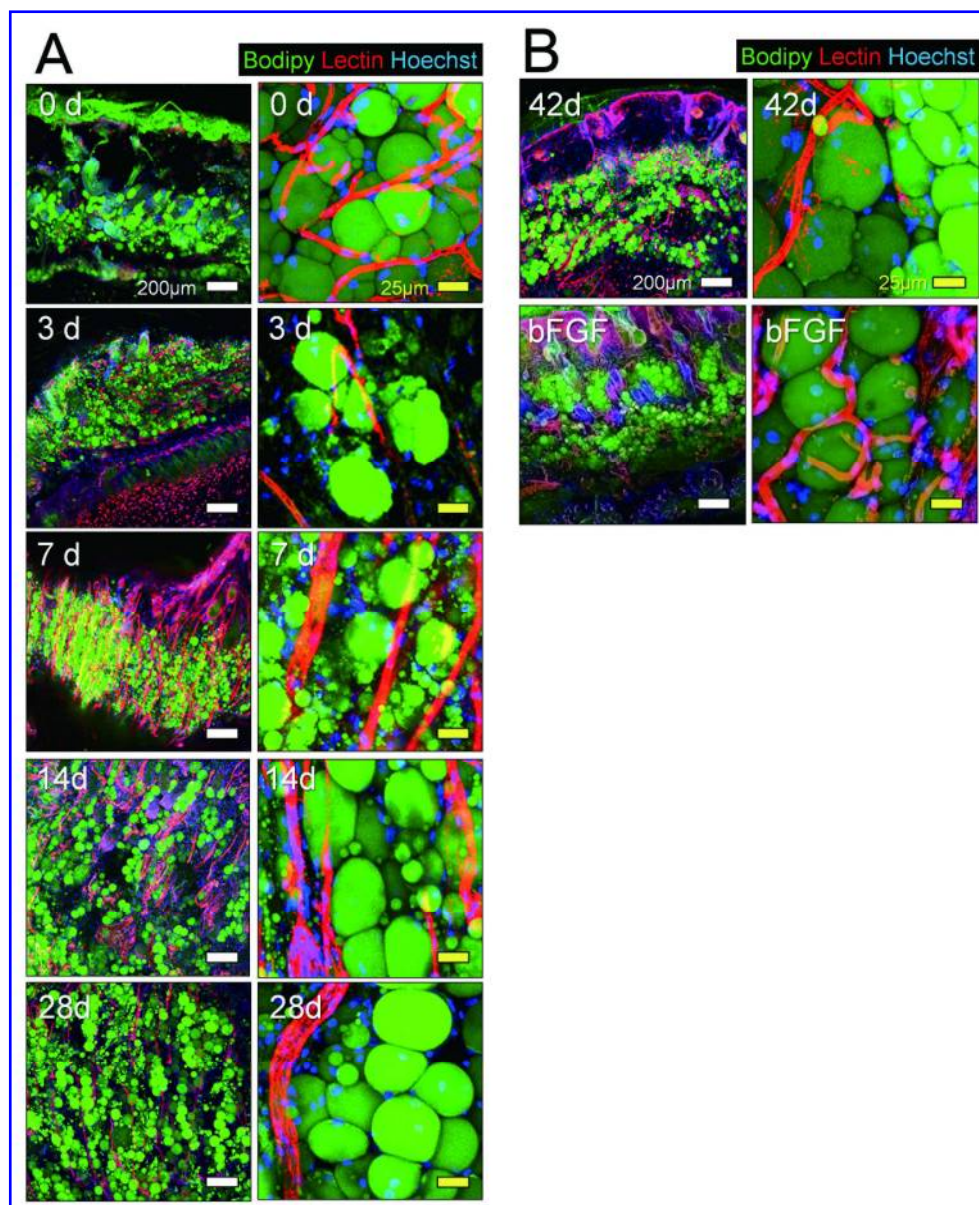


Figure 3. Whole mount histology of tissue samples

Harvested tissue was stained with BODIPY (adipocytes; green), lectin (endothelial cells; red), and Hoechst 33342 (nuclei; blue). (A) Suspended tissue samples at low (left column) or high (right column) magnification. With continuous suspension, the subcutaneous adipose layer thickened; numerous new capillaries formed in the adipose tissue and growth extended in the direction of the applied force. Scale bars = 200 μm (left column) or 25 μm (right column). (B) Tissue samples on day 42. The enlarged subcutaneous adipose tissue had shrunken by day 42 in controls; however, the administration of bFGF-incorporated microspheres was associated with a thicker layer of adipose and more prominent capillary network compared to the control. Scale bars = 200 μm (left column) or 25 μm (right column).

208x253mm (300 x 300 DPI)

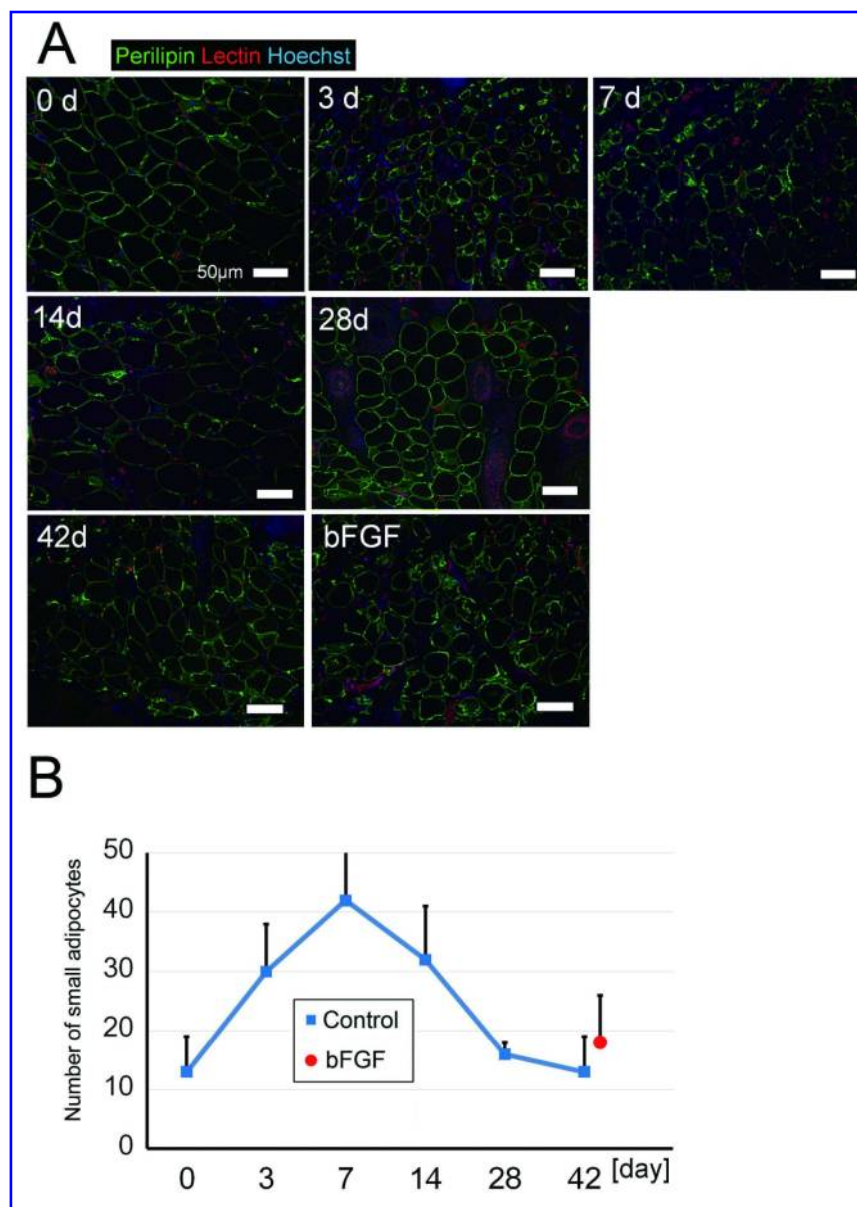


Figure 4. Measurement of small adipocytes in samples immunostained for perilipin. (A) Histological sections immunostained for perilipin (plasma membrane of viable adipocytes; green), or stained with lectin (endothelial cells; red) and Hoechst 33342 (nuclei; blue). Scale bars = 50 µm. (B) Sequential change in the number of small adipocytes. The numbers of small adipocytes (diameter of less than 30 µm) per optical field were counted. The number of small adipocytes, reflecting ongoing adipogenesis, peaked on day 7.

189x265mm (300 x 300 DPI)

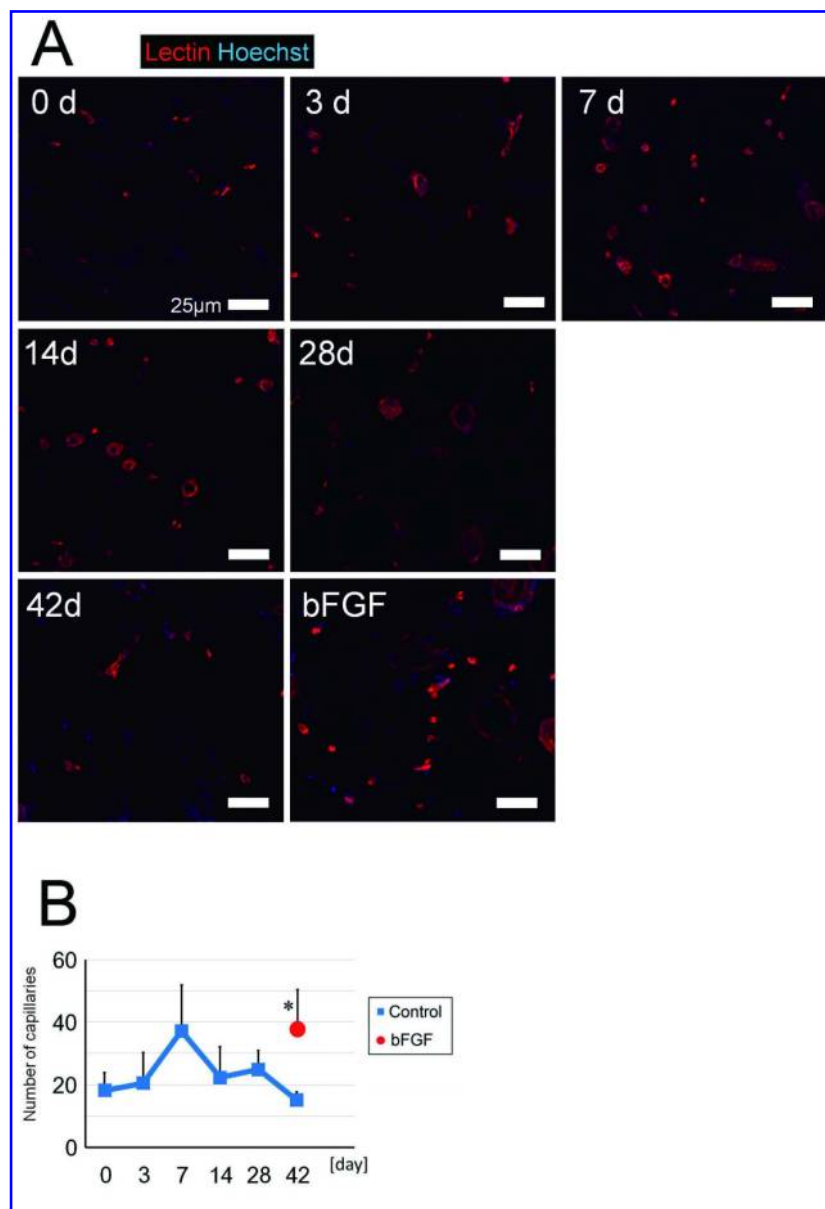


Figure 5. Histological measurement of vasculature in tissue samples
 (A) Histology of subcutaneous adipose tissue stained with lectin (endothelial cells; red) and Hoechst 33342 (nuclei; blue). Tissue was harvested on days 0, 3, 7, 14, and 28; some animals were removed from the suspension device and samples were harvested 14 days later (day 42). Some animals received bFGF-incorporated microspheres after removal of the suspension device, and then samples were harvested on day 42. Scale bars = 25 μ m. (B) Quantification of vessels in the subcutaneous adipose tissue. The number of vessels per field was counted in images at a low magnification. The largest number of vessels was observed on day 7. A larger number of vessels were counted in bFGF-treated tissues compared to the control on day 42 (* $p < 0.05$).

166x241mm (300 x 300 DPI)

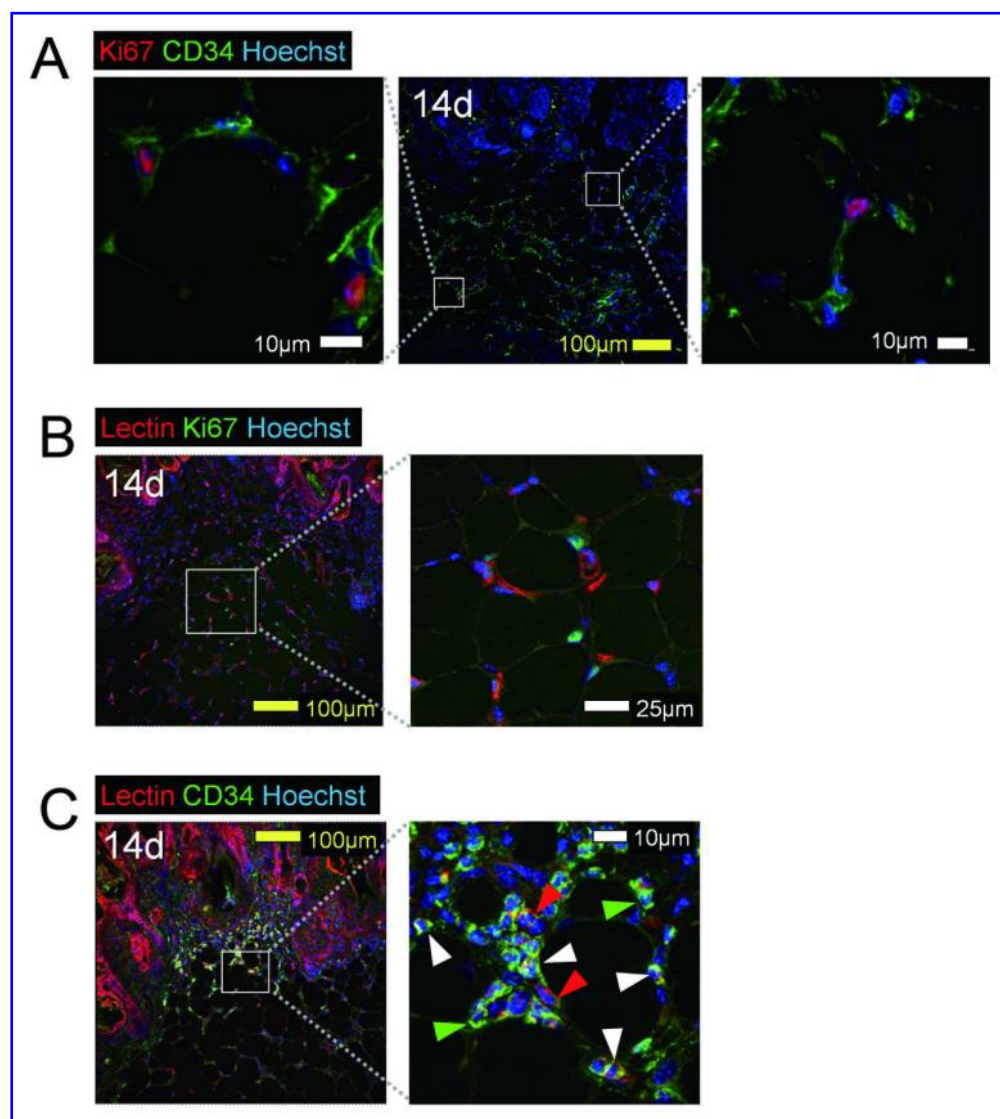


Figure 6. Immunohistological analysis of proliferating cells in tissues under suspension
 (A) Tissue samples harvested on day14 were triply stained with anti-Ki67 (proliferative cells; red), anti-CD34 (ASCs; green), and Hoechst 33342 (nuclei; blue). Most proliferating cells were CD34+, suggesting that they were ASCs. Scale bars = 100 μ m (yellow); boxed sections were enlarged at 10 μ m (white). (B) Tissue samples harvested on day14 were triply stained with lectin (capillaries; red), anti-Ki67 (proliferative cells; green), and Hoechst 33342 (nuclei; blue). Most of proliferating cells were lectin-, which also suggested that they were ASCs. Scale bars = 100 μ m (yellow); boxed section was enlarged at 25 μ m (white). (C) Tissue samples harvested on day14 were triply stained with lectin (capillaries; red), anti-CD34 (ASCs; green), and Hoechst 33342 (nuclei; blue). CD34+ cells were most frequently observed in the superficial adipose layer, immediately under the dermis. In that area, there were lectin+/CD34- endothelial cells (red arrow heads), lectin-/CD34+ ASCs (green arrow heads), and also lectin+/CD34+ cells (white arrow heads), which may be ASCs that are trans-differentiating into vascular endothelial cells. Scale bars = 100 μ m (yellow); boxed section was enlarged at 10 μ m (white).

177x196mm (300 x 300 DPI)

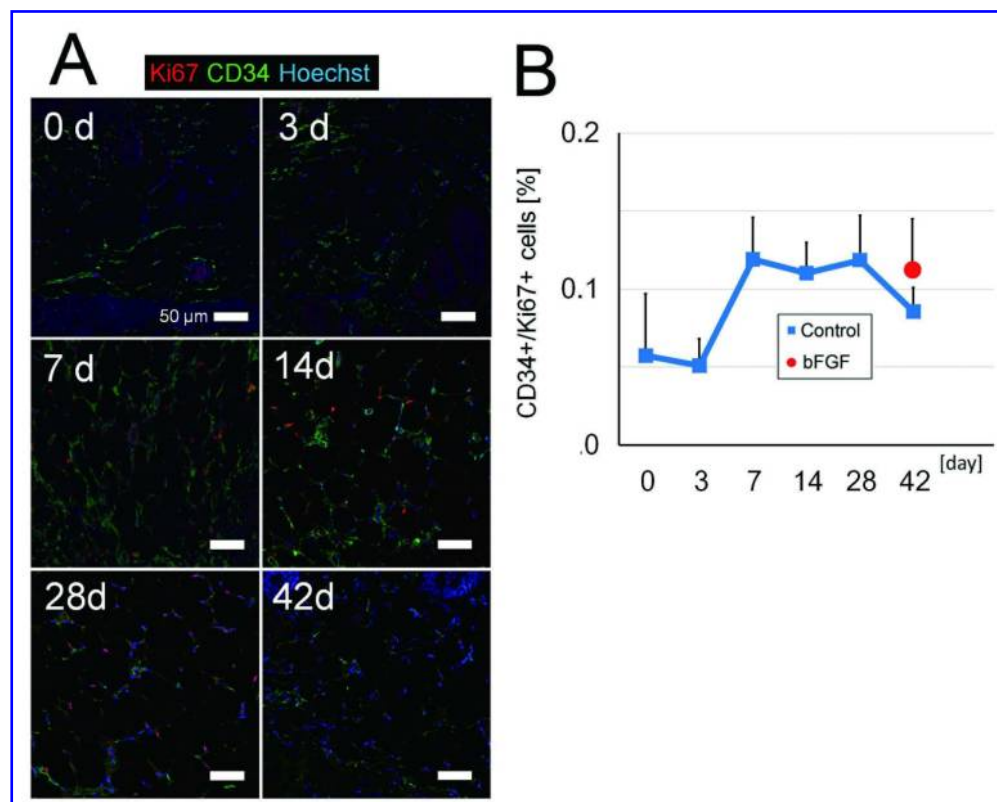
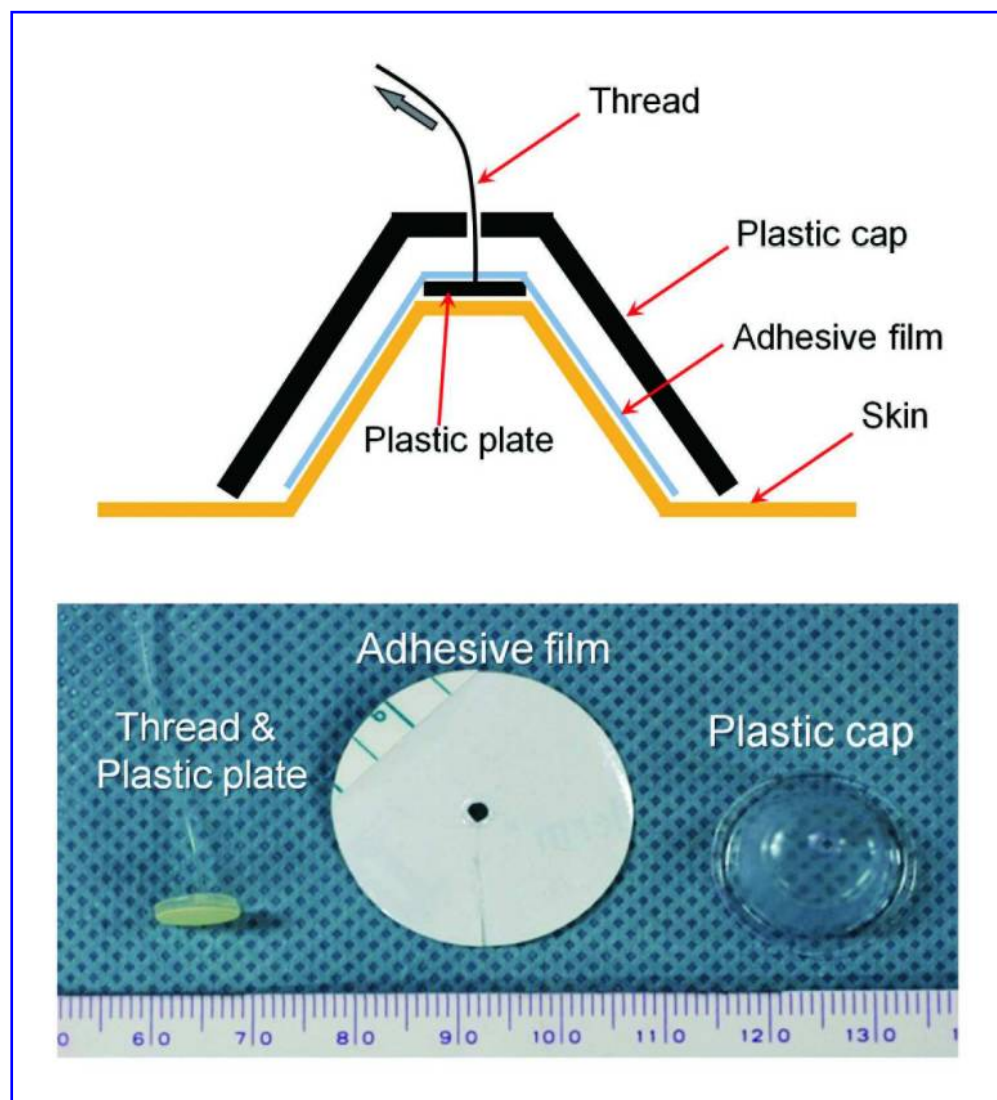


Figure 7. Histological measurement of proliferating ASCs in tissues under suspension
 (A) Tissue samples harvested on days 0, 3, 7, 14, 28, and 42 were triply stained with anti-Ki67 (proliferative cells; red), anti-CD34 (ASCs; green), and Hoechst 33342 (nuclei; blue). Scale bars = 50 μ m (B) Quantification of CD34+/Ki67+ cells. The double positive cells (ASCs) increased in number from day 7 to day 28. The number of proliferating ASCs decreased after cessation of suspension, but the decrease appeared to be partly compensated by administration of bFGF.

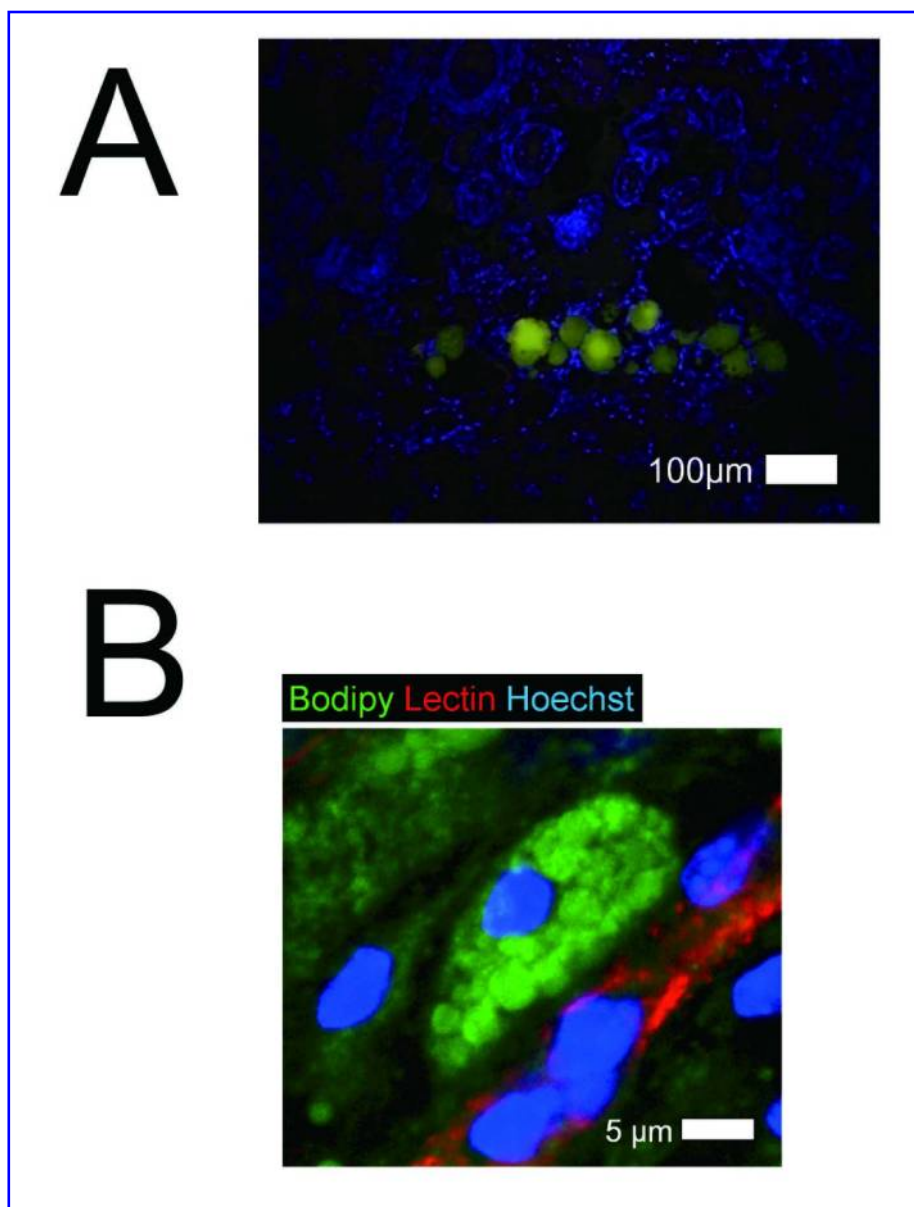
178x142mm (300 x 300 DPI)



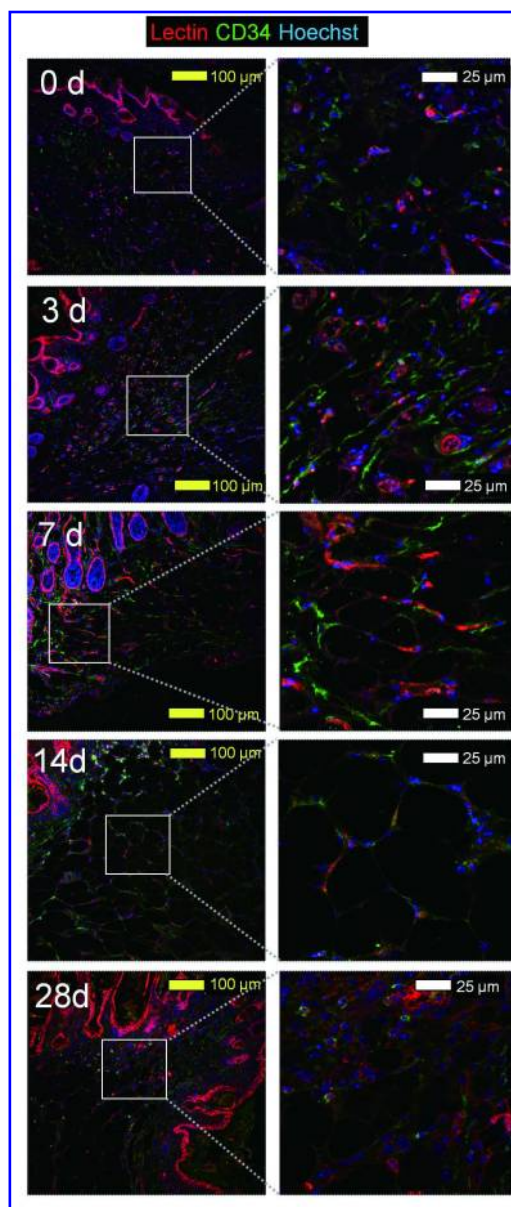
Supplementary Figure 1. Suspension device

A suspension device specifically designed for this experiment (Hiroki Corp., Yokohama, Japan). An adhesive film (diameter =30 mm) combined with a plastic plate was placed on the back skin of mice. A suspension thread attached to the plate was threaded through the hole in a plastic cap placed over the plate. The thread was then pulled upward and fixed to the plastic cap to maintain a suspending force on the skin (see also Figure 1A). The suspension device was exchanged every 5 days throughout the experiment.

126x138mm (300 x 300 DPI)

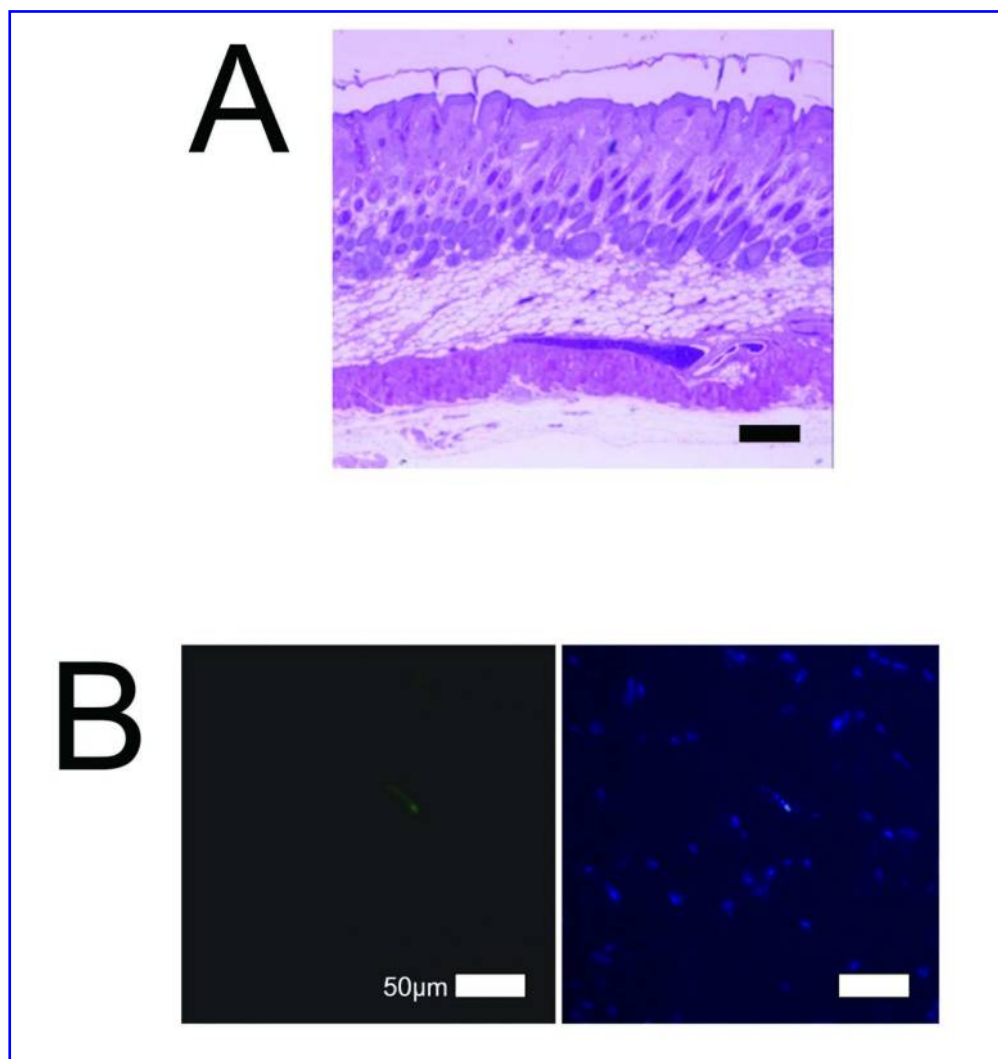


Supplementary Figure 2. The application of gelatin microspheres by subcutaneous injection. (A) Gelatin microspheres containing bFGF or PBS were subcutaneously injected on day 28, and tissue suspension was discontinued. A paraffin section of the harvested tissue was stained with DAPI (nuclei; blue) and the injected auto-fluorescent microspheres (yellow) were visualized under a fluorescence microscope. Scale bars = 100 µm. (B) Preadipocytes observed under external suspension (day 14). Whole mounts were triply-stained with BODIPY (lipid; green), lectin (endothelial cells; red), and Hoechst 33342 (nuclei; blue); preadipocytes located alongside the capillaries (red) contained numerous small lipid droplets (green). Scale bars = 5 µm.
131x172mm (300 x 300 DPI)



Supplementary Figure 3. Tissue samples were triply-stained with lectin (capillaries; red), anti-CD34 (ASCs; green), and Hoechst 33342 (nuclei; blue). Samples were harvested and stained on day 0, 3, 7, 14, and 28. Lectin+/CD34+ cells (white arrow heads), which may be cells that trans-differentiated from ASCs into vascular endothelial cells, were most frequently observed on day 14. Scale bars = 100 μm (yellow); boxed sections were enlarged at 25 μm (white).

103x243mm (300 x 300 DPI)



Supplementary Figure 4. Histological section of tissue samples harvested on day 29
(A) Hematoxylin and eosin staining of a sample harvested on day 29, one day after removal of the suspension device. A substantial reduction in tissue volume was observed compared to day 28. Scale bar = 200 μm . (B) TUNEL staining of tissue samples harvested on day 29. TUNEL staining (left column) and the same image merged with DAPI nuclear staining (right column) showed apoptotic changes. Scale bars = 50 μm .

169x178mm (300 x 300 DPI)